

Theoretical Study of the Structure and Vibrational Spectra of the $(\text{H}_2\text{O})_2 \cdots \text{HF}$ and $\text{H}_2\text{O} \cdots (\text{HF})_2$ Molecular Complexes

CARME ROVIRA AND PERE CONSTANS

*Grupo Química Cuántica, Dept. Química Física, Fac. Química,
Universitat de Barcelona, Av. Diagonal 647, 08028 Barcelona, Spain*

M.-H. WHANGBO

Chemistry Department, North Carolina State University, Raleigh, North Carolina 27695

JUAN J. NOVOA

*Grupo Química Cuántica, Dept. Química Física, Fac. Química,
Universidad de Barcelona, Av. Diagonal 647, 08028-Barcelona, Spain*

Abstract

Using the Hartree–Fock and MP2 methods with bases of up to 6-31++G(2d, 2p) quality, the optimum geometry of the 1:2 and 2:1 $(\text{H}_2\text{O})_n \cdots (\text{HF})_m$ complexes of water and hydrogen fluoride is searched in a systematic way. Two minimum-energy conformations are found for the 1:2 complex connected through a low-energy transition state. For the 2:1 complex, only one minimum-energy structure is obtained. The analysis of the geometries of the minima and their vibrational frequencies shows that none of them can be used to explain the existence of the $\text{H} \cdots \text{F} \cdots \text{H}$ reverse complex detected experimentally. © 1994 John Wiley & Sons, Inc.

Introduction

Understanding the structure and vibrational properties of the H_2O —HF heterodimer is important as a step in the study of the hydrogen bond. The infrared spectra of a mixture of HF and H_2O diluted in a matrix of Ar at 12 K shows the presence of three different hydrogen-bonded complexes [1], $\text{H}_2\text{O} \cdots (\text{HF})_2$, $\text{H}_2\text{O} \cdots \text{HF}$, and $\text{HF} \cdots \text{HOH}$, in increasing order of stability. The structure of these complexes are those shown in Figure 1: The $\text{H}_2\text{O} \cdots (\text{HF})_2$ dimer has an open structure $\text{H}_2\text{O} \cdots \text{HF} \cdots \text{HF}$; the $\text{H}_2\text{O} \cdots \text{HF}$ dimer has its only HF molecule, with the H atom pointing to one of the lone-pair orbitals of the oxygen atom, i.e., the HF behaves as an acid; finally, in the $\text{HF} \cdots \text{HOH}$ complex (identified by a H—F stretching at 3915.5 cm^{-1}), the HF molecule behaves as a base and is identified as the reverse complex. Although no data are reported on the $(\text{H}_2\text{O})_2 \cdots \text{HF}$ complex because they are masked by the strong $(\text{H}_2\text{O})_2$ absorptions, Andrews and Johnson [1] suggested in their infrared study that this complex should also be present in the mixture.

The aim of this work was to perform a systematic study on the structure, stability, and infrared spectra of the 1:2 and 2:1 complexes of water and hydrogen fluoride, i.e., the $\text{H}_2\text{O} \cdots (\text{HF})_2$ and $(\text{H}_2\text{O})_2 \cdots \text{HF}$ systems. Although the structure of the $\text{H}_2\text{O} \cdots \text{HF}$ complex is well understood in detail, both at the experimental [2–5] and theoretical levels [6–11], the amount of

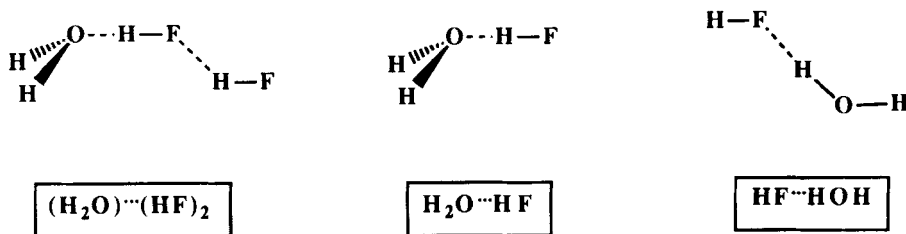


Figure 1. Proposed spectroscopic structures of the $\text{H}_2\text{O}\cdots(\text{HF})_2$, $\text{H}_2\text{O}\cdots\text{HF}$, and $\text{HF}\cdots\text{HOH}$ complexes.

information available for the other two complexes is rather limited [7, 12] and incomplete. Besides, as our previous study on the $\text{H}_2\text{O}\cdots\text{HF}$ complex [14] has shown that the reverse complex is not a minimum-energy structure in the potential energy surface of the dimer, we wanted to see if a $\text{H}\cdots\text{F}\cdots\text{H}$ motif can be found as a part of the geometry of the 1:2 or 2:1 trimers.

To perform our study, we employed *ab initio* methods that include a large extent of the electron correlation, using extended basis sets that give small basis set superposition errors on the whole potential energy surface. With this methodology, we performed a systematic search for the minimum-energy structures, and on these points, we carried out a vibrational analysis of the 1:2 and 2:1 complexes.

Method of Calculation

All computations reported here have been carried out using the Hartree–Fock (HF) and the second-order Møller–Plesset (MP2) methods. The MP2 method should give a good estimate of the correlation energy for these systems, as all of them have a large splitting between their HOMO and LUMO orbitals [13]. The search for the minimum-energy structures on the potential energy surface was done by choosing a set of representative structures and fully optimizing their structure using basis sets that provide a reasonably small basis-set superposition error (BSSE) [14]. BSSE was evaluated using the full counterpoise method [15]. Finally, vibrational frequencies and line intensities were computed at the MP2 level using the doubly harmonic approximation. All computations reported here were carried out using the algorithms included in the GAUSSIAN-92 program [16].

Results and Discussion

To locate all the minimum-energy structures on the potential energy surface for the $\text{H}_2\text{O}\cdots(\text{HF})_2$ and $(\text{H}_2\text{O})_2\cdots\text{HF}$ systems, we selected a set of representative geometrical arrangements using the empirical rules of Legon and Miller [17], hereafter identified as structures 1–8 (Fig. 2). Structures 1–5 are representative of the $\text{H}_2\text{O}\cdots(\text{HF})_2$ complex, whereas structures 6–8 correspond to the $(\text{H}_2\text{O})_2\cdots\text{HF}$ complex. On all of these structures we carried out a first optimization at the HF level using the STO-3G basis set. Then, the optimum HF/STO-3G structure was reoptimized at the HF/6-31G** level. In both optimizations, the geometry of the H_2O and HF fragments was frozen at their experimental values ($r_{\text{OH}} = 0.9584 \text{ \AA}$; $\angle\text{H—O—H} = 109.5^\circ$; $r_{\text{HF}} = 0.9568 \text{ \AA}$). The results from the optimizations (see Table I) show that the only minimum-energy structures for the $\text{H}_2\text{O}\cdots(\text{HF})_2$ complex are structures 4 and 5, in good agreement with the recent study of Hannachi et al. [18]. For

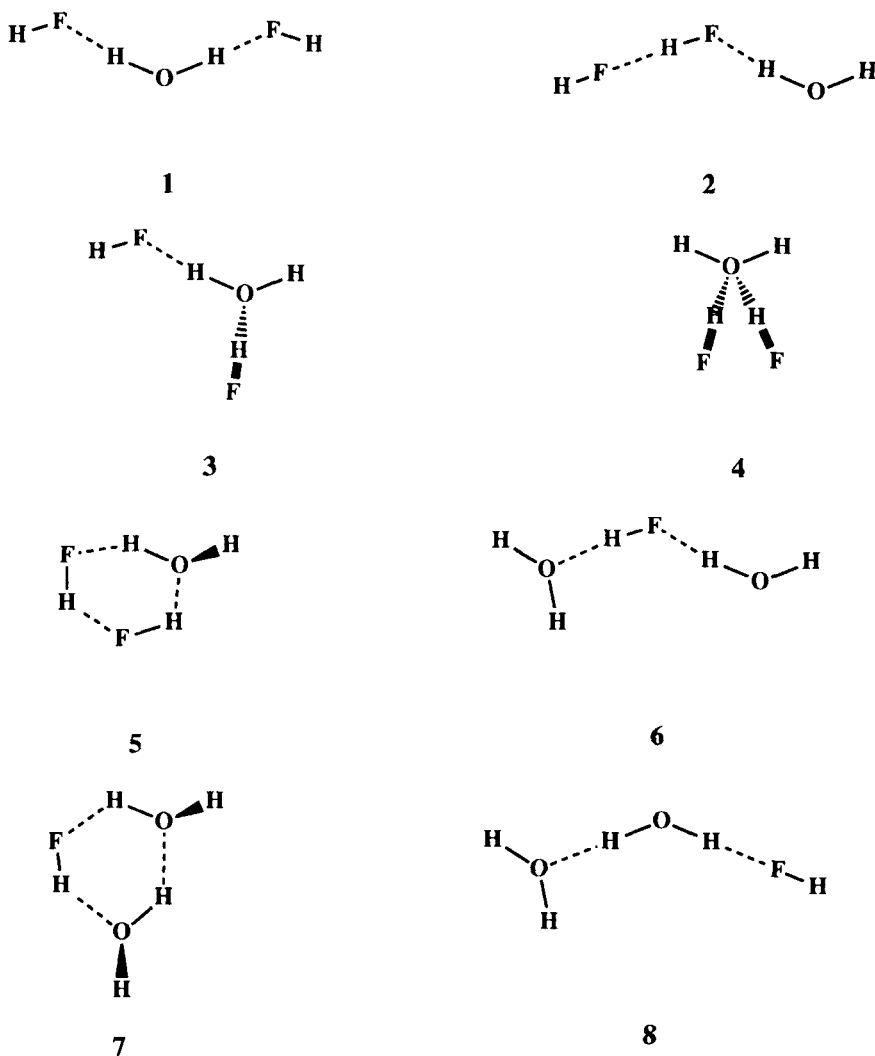


Figure 2. Geometrical arrangements employed in our calculations.

the $(\text{H}_2\text{O})_2 \cdots \text{HF}$ complex, the only minimum is structure **7**. These results show that, when the geometrical restrictions are raised, the trimer evolves to form the maximum number of hydrogen bonds. Note that there is no minimum in which there is a HF group acting only as a base. Either it plays an acid role as in structure **4** or has a dual acid–basic role. In consequence, there is no way the $\text{H} \cdots \text{F}—\text{H}$ motif can be found in the 1 : 2 or 2 : 1 $(\text{H}_2\text{O})_n \cdots (\text{HF})_m$ complexes. This fact is meaningful in describing the existence of a reverse complex, as will be shown later on.

A close look at the optimized geometries shows some interesting features: In structure **4**, the two HF molecules act as an acid, whereas in **5**, one acts as an acid and the other as a base. The geometry of **4** belongs to the C_{2v} symmetry group, with one plane being that of

TABLE I. Geometrical transformation of the spatial arrangements (see Fig. 2 for their description) during the optimization process.

Initial	Final
1	5
2	4
3	4
4	4
5	5
6	7
7	7
8	7

the water molecule and the other (at 90° relative to the first one) is the plane formed by the two HF molecules and the oxygen atom. In structures **5** and **7**, the system belongs to the C_1 point group. However, all atoms except the hydrogens of the water molecules not involved in a hydrogen bond (in arrangement **5** atom H_7 , and in arrangement **7**, atoms H_5 and H_8 ; see Fig. 3) lay close to the plane defined by the heavy atoms. It is worth noting here that atoms H_5 and H_8 of **7** are placed on the opposite sides of that imaginary plane. The fully optimized planar form of structures **5** and **7** show one and two imaginary frequencies, respectively, associated to motions that take H_7 or H_5 and H_8 out of the plane.

Once the optimum structures have been identified, we fully optimized their geometry at the HF and MP2 levels using as starting parameters the optimum HF/6-31G** values. In this step, the geometries of H_2O and HF were also included in the optimization. As the use of diffuse functions is known to play an essential role in the correct description of the hydrogen bond [19], we carried out these optimizations with the 6-31++G** and 6-31++G(2d,2p) basis sets at the HF level, whereas at the MP2 level, the only basis set used was the 6-31++G** set. The geometrical parameters obtained after the optimizations are included in Tables II, III, and IV, for structures **4**, **5**, and **7**, respectively. Table V gathers, for comparison, the optimum

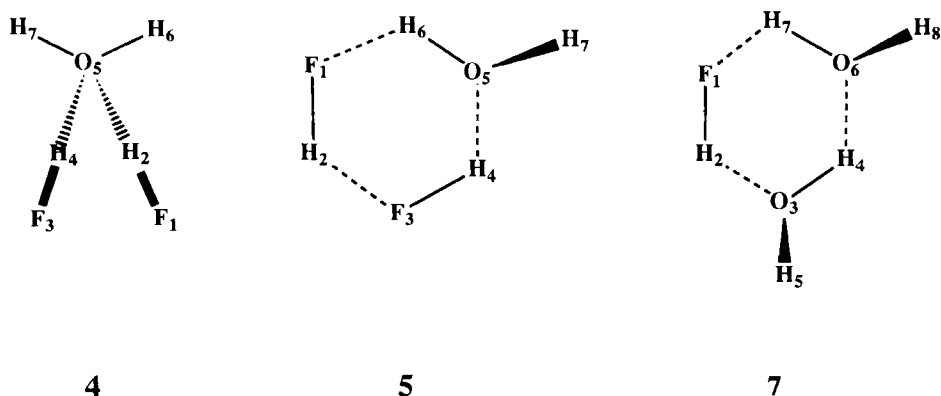
Figure 3. Atom numbering convention employed in the minimum energy structures **4**, **5**, and **7**.

TABLE II. Values of the nonequivalent geometrical parameters for the optimum-energy structure of arrangement 4 (see Fig. 3 for the numbering convention).

Parameter	HF			MP2
	6-31G**	6-31++G**	6-31++G(2d, 2p)	6-31++G**
F ₁ —H ₂	0.906	0.905	0.905	0.937
H ₂ —O ₅	1.896	1.894	1.894	1.804
O ₅ —H ₆	0.944	0.944	0.944	0.967
∠O ₅ H ₂ F ₁	166.3	171.2	172.5	172.5
∠H ₄ O ₅ H ₂	114.8	107.7	110.0	111.8
∠H ₇ O ₅ H ₆	106.8	106.6	106.6	105.7

$X_i—X_j$ indicates the distance between atoms X_i and X_j , and $\angle X_i X_j X_k$, the angle formed by atom X_i with the $X_j—X_k$ bond. The molecule belongs to the C_{2v} symmetry group with the two HF groups lying in a plane perpendicular to that formed by the water molecule. All distances are given in angstroms, and angles, in degrees.

TABLE III. Values of the geometrical parameters for the optimum-energy structure of arrangement 5 (see Fig. 3 for the numbering convention).

Parameter	HF			MP2
	6-31G**	6-31++G**	6-31++G(2d, 2p)	6-31++G**
F ₁ —H ₂	0.912	0.907	0.911	0.942
H ₂ —F ₃	1.786	1.851	1.870	1.765
F ₃ —H ₄	0.921	0.918	0.922	0.962
H ₄ —O ₅	1.734	1.730	1.736	1.610
O ₅ —H ₆	0.958	0.945	0.948	0.969
O ₅ —H ₇	0.943	0.941	0.944	0.964
H ₆ —F ₁	2.080	2.230	2.167	2.224
∠F ₃ H ₂ F ₁	150.0	150.9	148.0	149.6
∠H ₄ F ₃ H ₂	92.8	91.7	93.5	90.7
∠O ₅ H ₄ F ₃	154.3	160.9	157.8	160.8
∠H ₆ O ₅ H ₄	98.0	89.5	89.5	103.0
∠H ₇ O ₅ H ₄	123.0	124.6	129.4	122.4
∠H ₄ F ₃ H ₂ F ₁	-1.9	-2.2	-2.5	-1.9
∠O ₅ H ₄ F ₃ H ₂	0.4	2.3	2.1	-2.9
∠H ₆ O ₅ H ₄ F ₃	-2.6	-2.7	2.9	5.4
∠H ₇ O ₅ H ₄ F ₃	114.3	121.2	130.4	125.4

$X_i—X_j$ indicates the distance between atoms X_i and X_j ; $\angle X_i X_j X_k$, the angle formed by atom X_i with $X_j—X_k$ bond; and, finally, $\angle X_i X_j X_k X_l$, the dihedral angle formed by the X_i atom and the plane defined by the $X_j X_k X_l$ atoms, as measured from the $X_j X_k$ bond. All distances are given in angstroms, and angles, in degrees.

values of the intramolecular parameters of each isolated fragment with all basis sets and methods employed here. Figure 4 shows a tridimensional view of the optimized structures of structures 4, 5, and 7, respectively.

The analysis of the results included in Tables II–IV shows that, for the same method, the geometry of these systems does not change significantly from one basis set to another. The

TABLE IV. Values of the geometrical parameters for the optimum-energy structure of arrangement 7 (see Fig. 3 for the numbering convention).

Parameter	HF			MP2
	6-31G**	6-31++G**	6-31++G(2d, 2p)	6-31++G**
F ₁ —H ₂	0.919	0.917	0.921	0.958
H ₂ —O ₃	1.749	1.847	1.748	1.637
O ₃ —H ₄	0.952	0.949	0.951	0.976
O ₃ —H ₅	0.943	0.941	0.943	0.964
H ₄ —O ₆	2.000	2.062	2.038	1.916
O ₆ —H ₇	0.948	0.945	0.948	0.970
O ₆ —H ₈	0.943	0.940	0.943	0.963
H ₇ —F ₁	2.038	2.254	2.230	2.112
∠O ₃ H ₂ F ₁	157.6	162.1	161.0	161.6
∠H ₄ O ₃ H ₂	95.1	96.1	98.8	96.9
∠H ₅ O ₃ H ₂	119.8	121.4	124.8	121.0
∠O ₆ H ₄ O ₃	144.4	143.1	141.4	143.0
∠H ₇ O ₆ H ₄	90.7	98.0	98.1	97.2
∠H ₈ O ₆ H ₄	124.4	133.7	138.8	133.0
∠H ₄ O ₃ H ₂ F ₁	-4.4	-0.5	0.2	4.1
∠H ₅ O ₃ H ₂ F ₁	108.7	113.9	119.9	118.8
∠O ₆ H ₄ O ₃ H ₂	5.3	2.1	0.4	-1.4
∠H ₇ O ₆ H ₄ O ₃	-2.3	-2.8	-1.2	-1.3
∠H ₈ O ₆ H ₄ O ₃	-113.4	-125.3	-130.2	-121.8

X_i — X_j indicates the distance between atoms X_i and X_j ; $\angle X_i X_j X_k$, the angle formed by atom X_i with the X_j — X_k bond; and, finally, $\angle X_i X_j X_k X_l$, the dihedral angle formed by the X_i atom and the plane defined by the $X_j X_k X_l$ atoms, as measured from the $X_j X_k$ bond. All distances are given in angstroms, and the angles, in degrees.

most sensitive parameters turn out to be the intermolecular distances and the angles. Our values also reflect the effect that the hydrogen-bond formation causes on the intramolecular bonds of each fragment. This is seen in the asymmetry of the two O—H bonds of each water molecule and in the different values of the H—F distance in the HF molecules of each arrangement, as corresponds to their different environments. Inclusion of electron correlation decreases the length of the hydrogen bonds and increases the bond lengths in each fragment, as expected.

To be able to correlate our data with the experimental data, we have to know the relative stability of those systems and the barrier between the different isomers of the same compound. Table V reports for structures 4, 5, and 7 the total energy (E , in atomic units), the interaction energy (ΔE in kcal/mol), the value estimated by the full counterpoise method for the basis-set superposition error (BSSE, in kcal/mol), the BSSE-corrected value of the interaction energy (ΔE_{cp} , in kcal/mol), and, finally, the interaction energy corrected by the BSSE and the zeroth-point energy (ΔE_{zpe} , in kcal/mol). The last property has been estimated using the values of the vibrational frequencies computed using the harmonic approximation. According to the values of the interaction energy, structure 4 is the least stable one, whereas structures 5 and 7 have a similar stability. This result can be rationalized in the following way: Structure 4 has two F—H \cdots O hydrogen bonds, whereas structures 5 and 7 both have three hydrogen bonds of similar magnitude: The first has one F—H \cdots O, one O—H \cdots F, and one F—H \cdots F bond, and the second has one F—H \cdots O, one O—H \cdots F, and one O—H \cdots O bond. The strength

TABLE V. Total energy (E , in atomic units), interaction energy (ΔE , in kcal/mol), basis-set superposition error (BSSE, in kcal/mol), interaction energy corrected by the BSSE (ΔE_{cp} , in kcal/mol), and interaction energy corrected by the BSSE and the zeroth-point energy (ΔE_{ZPE} , in kcal/mol) computed at the optimum-energy structure of arrangements 4, 5, and 7.

Property	HF			MP2 ^a 6-31++G**
	6-31G**	6-31++G**	6-31++G(2d, 2p)	
Arrangement 4				
E	-276.070569	-276.101370	-276.111823	-276.691140
ΔE	-14.79	-13.45	-12.04	-16.27
BSSE	2.28	0.02	0.71	3.00
ΔE_{cp}	-12.51	-13.47	-11.33	-13.27
ΔE_{ZPE}	-9.86	-8.58	-7.24	-11.34
Arrangement 5				
E	-276.080714	-276.105555	-276.116090	-276.696534
ΔE	-21.16	-16.08	-14.72	-19.65
BSSE	5.14	0.41	0.31	2.40
ΔE_{cp}	-16.02	-16.49	-14.41	-17.25
ΔE_{ZPE}	-15.39	-11.00	-9.55	-14.23
Arrangement 7				
E	-252.091118	-252.113207	-252.124679	-252.715641
ΔE	-20.24	-16.49	-14.36	-20.69
BSSE	4.29	1.03	0.38	-3.11
ΔE_{cp}	-15.95	-15.46	-13.97	-17.58
ΔE_{ZPE}	-14.27	-11.09	-9.18	-14.95

^aComputed freezing the core orbitals.

of the O—H⋯O and F—H⋯F is known to be similar in the water dimer and the hydrogen fluoride dimer (the MP2/6-311++G(2d, 2p) interaction energy for (H₂O)₂ and (HF)₂ is -5.44 and -5.00 kcal/mol without BSSE corrections, respectively [20]), so it is not at all surprising to obtain the same result when one substitutes a water molecule by a HF molecule in a similar environment, as is the case of structures 5 and 7.

Another interesting aspect of the interaction energies is the so-called cooperative effect, i.e., the difference between the value of the interaction energy of the trimer and that of each dimer ($E_{coop} = \Delta E_{abc} - \Delta E_{ab} - \Delta E_{bc} - \Delta E_{ca}$) caused by the mutual polarization of the monomer wavefunctions. Taking as values for $\Delta E_{\text{water-HF}}$, $\Delta E_{\text{water-water}}$ and $\Delta E_{\text{HF-HF}}$, the values for the interaction energies of the water-HF, water-water, and HF-HF systems computed with the MP2 method and the 6-311++G(2d, 2p) basis set (-7.87 [14], -5.00 [20], and -5.40 [20] kcal/mol, respectively), one can obtain for structures 5 and 7 an MP2 estimate for E_{coop} of -1.38 and -2.41 kcal/mol, respectively, from the values reported in Table V. These values must be taken as a measure of the importance of the mutual polarization; better numerical estimates require the computation ΔE_{ab} , ΔE_{bc} , and ΔE_{ca} with all coordinates frozen in the trimer geometry using the same basis set employed to compute ΔE_{abc} for the trimer.

To complete our analysis of the relative stability of the two forms of the 1:2 complex (structures **4** and **5**), we have computed the energetic barrier for the transition from one structure to the other. The transition state for that process was computed by doing a systematic search on the potential energy surface along the possible pathways from **5** to **4**. The lowest possible pathway can be described as the rotation of the F_1-H_2 monomer, breaking the $H_2 \cdots F_3$ and $H_6 \cdots F_1$ intermolecular bonds while simultaneously creating the $H_2 \cdots O_5$ intermolecular bond. During that process, the water molecule also rotates along the H_6-O_5 bond out of the plane. Once the point was located, its transition state nature on the potential energy surface was tested, computing the number of negative eigenvalues of the Hessian. The transition-state geometry is represented in Figure 5. Its total energy is -276.069103 atomic units at the HF/6-31G** level. Therefore, the transition state is located in the vicinity of structure **4** and the barrier for the $4 \rightarrow 5$ process is only 0.92 kcal/mol, whereas that for the $5 \rightarrow 4$ process is 7.29 kcal/mol (at the HF/6-31G** level). Therefore, at the low temperature in which the infrared spectra is measured, we can expect that most of the 1:2 molecules will be in the cyclic form **5** instead of the open form **4**. We do not expect that the inclusion of correlation at

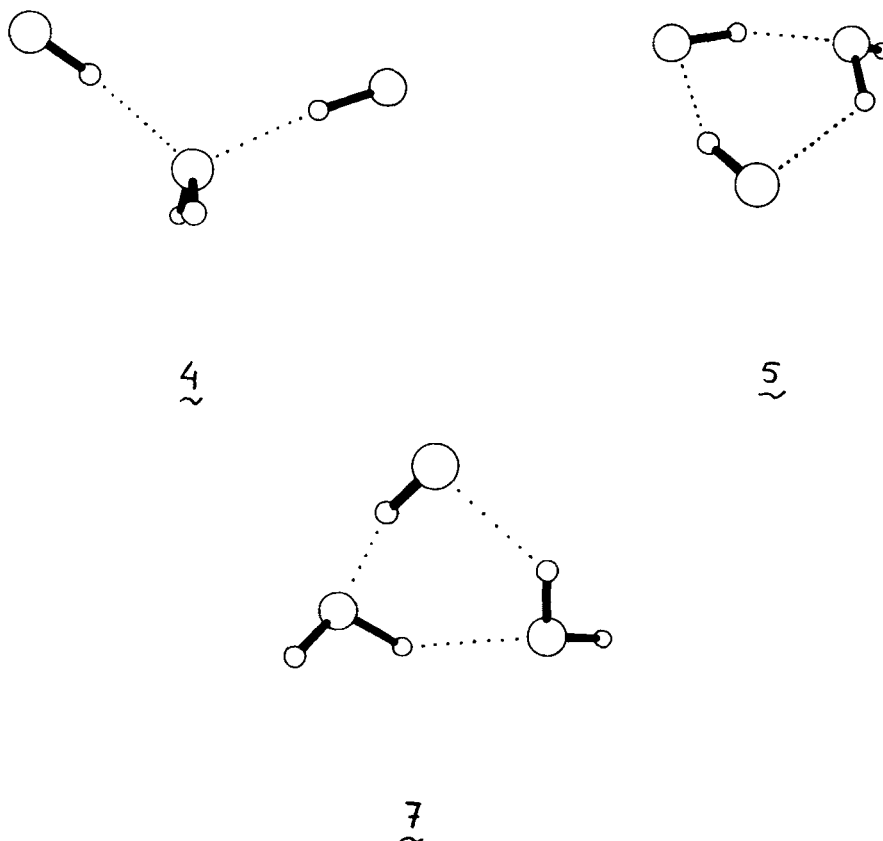


Figure 4. Tridimensional representation of the optimum geometry of structures **4**, **5**, and **7**.

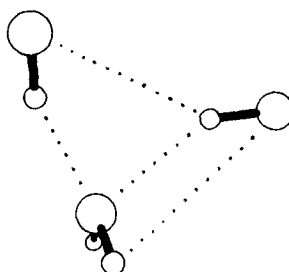


Figure 5. Tridimensional representation of the optimum geometry of the transition state of lowest-energy connecting structures **4** and **5**

the MP2 level modifies the previous conclusions very much given the large energy difference between structures **4** and **5** also present at that level (see Table V).

The final step of our calculation has been the vibrational analysis of the optimized structures. We carried out this analysis at the HF and MP2 levels using the basis sets included in Tables VII–IX. We have also included in Table VI the results for the monomers to allow for comparisons.

TABLE VI. Optimum geometry (X – Y distances in angstroms, $\angle XYZ$ angles in degrees), total energy (E , in atomic units), vibrational frequencies (ν_i , in cm^{-1}) and their IR intensities (given in parentheses in km/mol), and zero-point energy (ZPE, in kcal/mol) computed using the Hartree–Fock (HF) and MP2 methods for the isolated HF and H₂O molecules.

Property	HF			MP2 ^a
	6-31G**	6-31++G**	6-31++G(2d, 2p)	6-31++G**
HF molecule				
H—F	0.900	0.902	0.898	0.926
E	–100.011691	–100.024312	–100.027820	–100.215919
ν_{HF}	4493 (133)	4473 (176)	4472 (165)	4119 (126)
ZPE	6.42	6.39	6.39	5.89
H₂O molecule				
O—H	0.943	0.943	0.941	0.963
$\angle \text{HOH}$	105.9	107.1	106.1	105.3
E	–76.023615	–76.031309	–76.036990	–76.233376
ν_a^a	4262 (58)	4269 (89)	4259 (88)	4010 (10)
ν_s^b	4145 (16)	4147 (20)	4150 (19)	3863 (9)
ν_b^c	1770 (104)	1728 (114)	1758 (100)	1620 (89)
ZPE	14.55	14.50	14.53	13.57

^aH₂O antisymmetric stretching.

^bH₂O symmetric stretching.

^cH₂O bending.

TABLE VII. Harmonic vibrational frequencies (in cm^{-1}), IR intensities (in km/mol), and zero-point energy (ZPE, in kcal/mol) computed for the optimum structure of arrangement 4 using the Hartree–Fock and MP2 methods.

Property	HF			MP2
	6-31G**	6-31++G**	6-31++G(2d, 2p)	6-31++G**
1 (A_1)	32 (12)	35 (9)	35 (8)	33 (10)
2 (B_1)	117 (0)	167 (0)	165 (1)	144 (1)
3 (A_1)	167 (2)	169 (1)	166 (0)	184 (0)
4 (B_2)	187 (0)	190 (1)	185 (1)	212 (1)
5 (A_2)	199 (19)	235 (0)	245 (0)	231 (0)
6 (B_2)	251 (113)	293 (77)	306 (89)	314 (85)
7 (A_1)	590 (359)	622 (337)	627 (277)	653 (296)
8 (B_2)	647 (245)	672 (336)	653 (271)	712 (253)
9 (A_2)	690 (414)	705 (0)	705 (0)	753 (0)
10 (B_1)	690 (0)	738 (455)	713 (370)	782 (390)
11 (A_1)	1766 (121)	1752 (125)	1767 (110)	1636 (98)
12 (A_1)	4116 (81)	4107 (96)	4110 (86)	3820 (160)
13 (B_1)	4226 (152)	4217 (173)	4211 (160)	3851 (1066)
14 ^a (B_2)	4332 (837)	4279 (923)	4274 (160)	3897 (229)
15 ^b (A_1)	4359 (145)	4309 (280)	4303 (280)	3957 (144)
ZPE	31.99	32.15	32.11	30.28

^aHF symmetric stretching.^bHF antisymmetric stretching.TABLE VIII. Harmonic vibrational frequencies (in cm^{-1}), IR intensities (in km/mol), and zero-point energy (ZPE, in kcal/mol) computed for the optimum structure of arrangement 5 using the Hartree–Fock and MP2 methods.

Property	HF			MP2
	6-31G**	6-31++G**	6-31++G(2d, 2p)	6-31++G**
1	161 (10)	84 (16)	83 (15)	111 (17)
2	219 (94)	166 (115)	176 (79)	209 (4)
3	224 (17)	185 (10)	189 (9)	218 (94)
4	265 (6)	241 (12)	245 (9)	275 (15)
5	326 (63)	301 (86)	307 (102)	355 (82)
6	516 (246)	407 (146)	419 (155)	477 (204)
7	546 (88)	507 (96)	531 (89)	583 (99)
8	669 (374)	569 (365)	585 (315)	654 (344)
9	808 (405)	777 (404)	807 (303)	902 (300)
10	1057 (123)	998 (170)	1010 (138)	1117 (144)
11	1776 (112)	1746 (121)	1766 (103)	1646 (89)
12 ^a	4019 (579)	4008 (797)	3988 (819)	3374 (1111)
13	4108 (168)	4115 (65)	4113 (61)	3807 (168)
14	4234 (155)	4242 (156)	4228 (140)	3823 (465)
15 ^b	4269 (541)	4283 (513)	4273 (517)	3969 (154)
ZPE	33.16	32.36	32.48	30.77

^aH₄—F₃ stretching.^bH₂—F₁ stretching.

TABLE IX. Harmonic vibrational frequencies (in cm⁻¹), IR intensities (in km/mol), and zero-point energy (ZPE, in kcal/mol) computed for the optimum structure of arrangement **7** using the Hartree–Fock and MP2 methods.

Property	HF			MP2
	6-31G**	6-31++G**	6-31++G(2d, 2p)	6-31++G**
1	159 (9)	102 (11)	100 (7)	127 (11)
2	186 (183)	141 (169)	145 (142)	196 (164)
3	203 (1)	186 (7)	171 (11)	215 (11)
4	253 (6)	235 (13)	188 (5)	266 (5)
5	271 (89)	246 (125)	248 (117)	293 (111)
6	308 (16)	293 (38)	276 (35)	326 (69)
7	382 (72)	355 (80)	352 (77)	388 (72)
8	548 (321)	438 (187)	426 (186)	500 (189)
9	647 (265)	582 (246)	577 (227)	658 (249)
10	806 (359)	802 (366)	789 (263)	903 (274)
11	1016 (114)	972 (189)	924 (150)	1077 (162)
12	1785 (141)	1748 (194)	1768 (160)	1640 (154)
13	1789 (77)	1758 (39)	1777 (34)	1653 (21)
14 ^a	4015 (158)	4016 (489)	4031 (275)	3440 (1001)
15	4081 (472)	4068 (466)	4074 (516)	3703 (345)
16	4111 (399)	4112 (160)	4112 (169)	3805 (117)
17	4224 (124)	4231 (160)	4220 (142)	3954 (129)
18	4236 (140)	4247 (155)	4236 (143)	3974 (126)
ZPE	41.49	40.79	40.63	38.77

^aHF stretching.

The analysis of the vibrational frequencies shows the presence of two types of vibrational modes: a first group of low vibrational frequencies, associated to the intermolecular vibrations, and a second group containing intramolecular normal modes, at frequencies very close to the values in the isolated fragments. The results are slightly affected by the addition of diffuse functions or polarization to the basis set; however, inclusion of correlation influences results to a greater extent, in particular, these of intramolecular modes.

Of particular importance among intramolecular normal modes is the position of the HF stretching. Looking at the MP2 values, in all complexes its value is shifted to lower frequencies, as expected. The extent of the shift is known to be proportional to the value of the interaction energy and this is the result found in our case. In this way, the symmetric and asymmetric HF stretching of **4** and the H₂—F₁ stretching in **5** lie close to 3900 cm⁻¹. However, their intensity is small. In contraposition, the H₄—F₃ stretching of **5** and the H₂—F₁ of **7** both are located at much lower values (around 3400 cm⁻¹) and their intensity is very high. The first set of values is similar to the HF stretching in the (HF)₂ complex, whereas the second set is also similar to the O—H stretching in the (H₂O)₂ complex. It is also important to note that the computed harmonic MP2 values are expected to be an overestimation of the experimental results (for the H₂O and HF monomers, the error in the stretchings are about 200 cm⁻¹) [20]. Therefore, our calculations give results for the HF stretching smaller than those compatible with an experimental value of 3915.5 cm⁻¹. Such a value can be associated only with weaker interactions of a HF monomer of the type expected in a reverse complex, i.e., with a HF acting

purely as a base. However, the results shown above on the minimum-energy structures allow us to conclude that there is no such a type of structure in the 1:2 and 2:1 complexes of water and HF.

Concluding Remarks

Our Hartree–Fock and MP2 results on the structure of the 1:2 and 2:1 $(\text{H}_2\text{O})_n \cdots (\text{HF})_m$ complexes of water and hydrogen fluoride have allowed us to obtain useful information for the interpretation of infrared spectra of water and hydrogen fluoride mixtures. Two minimum-energy conformations have been found for the 1:2 complex, connected through a low-energy transition state. For the 2:1 complex, only one minimum-energy structure has been obtained. The analysis of the geometries of these minima shows that none of them presents the $\text{H} \cdots \text{F}—\text{H}$ motif in their structure. The vibrational analysis indicates that the 3915.5 cm^{-1} frequency, characteristic of a $\text{H}—\text{F}$ stretching of the reverse complex, cannot be associated to any of the computed minima. Therefore, the structure of the so-called reverse complex is still an unsolved problem.

Acknowledgments

This work was supported by the U.S. Department of Energy, Office of Basic Energy Sciences, Division of Materials Science, under Grant DE-FG05-86ER45259 and by the Spanish DGICYT under projects PB89-0268 and PB92-0655-C02-02. We express our appreciation for the allocation of computer time on the CRAYs made available by DOE and CESCA, the Center of Supercomputation of Catalunya (Spain). C. R. and P. C. also want to thank the Generalitat de Catalunya for their doctoral grants.

Bibliography

- [1] L. Andrews and G. L. Johnson, *J. Chem. Phys.* **79**, 3670 (1983).
- [2] R. K. Thomas, *Proc. R. Soc. Lond. Ser. A* **344**, 579 (1975).
- [3] J. W. Bevan, Z. Kisiel, A. C. Legon, D. J. Millen, and S. C. Rogers, *Proc. R. Soc. Lond. Ser. A* **372**, 441 (1980).
- [4] Z. Kisiel, A. C. Legon, and D. J. Millen, *Proc. R. Soc. Lond. Ser. A* **381**, 419 (1982).
- [5] Z. Kisiel, A. C. Legon, and D. J. Millen, *J. Chem. Phys.* **78**, 2910 (1983).
- [6] A. Hinchliffe, *J. Mol. Struct. (Theochem)* **106**, 361 (1984).
- [7] M. M. Szczesniak, S. Scheiner, and Y. Boutellier, *J. Chem. Phys.* **81**, 5024 (1984).
- [8] J. A. Del Bene, *J. Chem. Phys.* **92**, 2874 (1988).
- [9] R. D. Amos, J. F. Gaw, N. C. Handy, E. D. Simandiras, and K. Somasundram, *Theor. Chim. Acta* **71**, 41 (1987).
- [10] Y. Hannachi, B. Silvi, and Y. Boutellier, *J. Chem. Phys.* **94**, 2915 (1991).
- [11] Y. Hannachi, B. Silvi, J. P. Perchard, and Y. Boutellier, *Chem. Phys.* **154**, 23 (1991).
- [12] J. C. Drill, L. C. Allen, W. C. Topp, and J. A. Pople, *J. Am. Chem. Soc.* **97**, 7220 (1975).
- [13] J. J. Novoa, *J. Chem. Phys.* **94**, 4835 (1991).
- [14] J. J. Novoa, M.-H. Whangbo, and J. M. Williams, submitted.
- [15] S. F. Boys and F. Bernardi, *Mol. Phys.* **19**, 553 (1970).
- [16] M. J. Frisch, J. S. Binkley, H. B. Schlegel, K. Ragavachari, C. F. Melius, R. L. Martin, J. J. P. Stewart, F. W. Bobrowicz, C. M. Rohlfing, L. R. Kahn, D. J. Defrees, R. Seeger, R. A. Whiteside, D. J. Fox, E. M. Fleuder, J. A. Pople, GAUSSIAN-86 (Carnegie-Mellon, Quantum Chemistry Publishing Unit, Pittsburgh, 1984).
- [17] A. C. Legon and D. J. Millen, *Chem. Rev.* **6**, 635 (1986).
- [18] Y. Hannachi, B. Silvi, and Y. Boutellier, *J. Chem. Phys.* **97**, 1911 (1992).

- [19] (a) J. J. Novoa, B. Tarron, M.-H. Whangbo, and J. M. Williams, *J. Chem. Phys.* **95**, 5179 (1991). (b) S. Scheiner, in *Reviews in Computational Chemistry*, K. Lipkowitz and D. Boyd, Eds. (VCH, New York, 1991), Vol. 2, and references therein.
- [20] M. J. Frisch, J. E. Del Bene, J. S. Binkley, and H. F. Schaefer III, *J. Chem. Phys.* **84**, 2279 (1986).

Received June 29, 1993

Accepted for publication January 24, 1994